ACS APPLIED BIO MATERIALS Article
Cite This: ACS Appl. Bio Mater. 2018, 1, 561−571
www.acsabm.org

# Design of Mucoadhesive PLGA Microparticles for Ocular Drug Delivery

Dawei Ding,[†] Binu Kundukad,[†] Ambika Somasundar,[‡] Sindhu Vijayan,[§] Saif A. Khan,*[,†,‡] and Patrick S. Doyle*[,†,∥]

[†]BioSystems and Micromechanics (BioSyM) IRG, Singapore-MIT Alliance for Research and Technology (SMART) Centre, 1 CREATE Way, Enterprise Wing, Singapore 138602, Singapore

[‡]Department of Chemical and Biomolecular Engineering, National University of Singapore,4 Engineering Drive 4, Singapore 117576, Singapore

[§]Pillar of Engineering Product Development, Singapore University of Technology and Design, 8 Somapah Road, Singapore 487372, Singapore

[∥]Department of Chemical Engineering, Massachusetts Institute of Technology, 25 Ames Street, Building 66, Cambridge, Massachusetts 02139, United States

Supporting Information

**ABSTRACT:** Topically administered ocular drug delivery systems typically face severe bioavailability challenges because of the natural protective mechanisms of eyes. The rational design of drug delivery systems that are able to persist on corneal surfaces for sustained drug release is critical to tackle this problem. In this study, we fabricated monodisperse chitosan-coated PLGA microparticles with tailored diameters from 5 to 120 $\mu$m by capillary microfluidic techniques and conducted detailed investigations of their mucoadhesion to artificial mucin-coated substrates. AFM force spectroscopy revealed strong instant adhesion to mucins, whereas the adhesion force, rupture length, and adhesion energy were positively correlated to the particle diameter and contact time. Particle detachment tests under shear flow in a microfluidic mucin-coated flow cell were in accord with the AFM measurements and revealed that microparticles smaller than 25 $\mu$m exhibited strong persistence in the flow cell, withstanding high shear rates up to 28,750 $s^{-1}$ which are equivalent to the harshest in vivo ocular conditions. A simple scaling analysis connects the AFM and detachment tests, and reveals the existence of a threshold diameter below which mucoadhesion performance essentially saturates—an important insight in managing the opposing design criteria of enhanced mucoadhesion and slow, sustained drug delivery. Our findings thus pave the way for the rational design of mucoadhesive microparticulate ocular drug delivery systems that are capable of enhancing the bioavailability of topically applied drugs to eyes, as well as to other tissues whose epithelial surfaces contain mucosae.

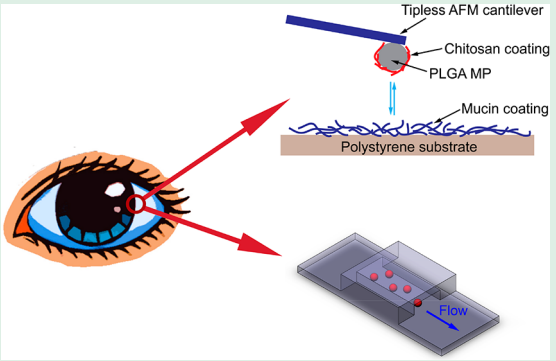


**KEYWORDS:** *mucoadhesion, drug delivery, microfluidics, chitosan, AFM, particle size, shear test*

## 1. INTRODUCTION

Visual impairment is currently estimated to affect over 285 million people worldwide.[1] Treatment of eye diseases such as glaucoma has been investigated for many decades, and many therapeutic methods have been established, which include noninvasive topical drug administration in formulations such as gels, ointments and eye drop solutions, and invasive methods such as surgical inserts and injections.[2] At present, topical formulations are the preferred route for ocular drug delivery because of the ease of administration and high patient compliance. Of these, eye drops represent more than 90% of the available commercial formulations.[3] Nevertheless, the unique anatomy and physiology of the eye presents a major challenge in topical ocular drug delivery. The natural defense mechanisms of eyes (e.g., tear dilution, nasolacrimal drainage, and reflex blinking) keep foreign materials away from entering the eye, thereby limiting the bioavailability of topically administered drugs.[3] Only 1−3% of topically instilled drugs typically reach the target intraocular tissue, thus limiting their therapeutic efficacies.[4] Concomitantly, the high frequencies of dosage necessitated by limited bioavailability present a major hurdle for patient compliance.[5] There has consequently been much interest in polymeric mucoadhesive particulate drug delivery systems to overcome some of these challenges.[6] Besides the advantage of controlled drug release,[7] these systems leverage the presence of mucosal layers in the tear

Received: April 25, 2018
Accepted: August 15, 2018
Published: August 16, 2018






DOI: 10.1021/acsabm.8b00041
ACS Appl. Bio Mater. 2018, 1, 561−571

Table 1. Characteristics and Tunability of PLGA Droplets and MPs Produced by Capillary Microfluidics

| | nozzle size | PLGA concentration/flow rate (μL/min) | PVA concentration/flow rate (μL/min) | droplet size (μm) | particle diameter (μm) |
|---|---|---|---|---|---|
| a | 220 μm | 1%, 20 | 2%, 100 | ∼550 | 122.7 ± 2.1 |
| b | | 0.1%, 15 | 2%, 90 | ∼550 | 63.0 ± 1.5 |
| c | | 1%, 15 | 4%, 90 | ∼150 | 38.6 ± 0.8 |
| d | | 1%, 15 | 6%, 90 | ∼100 | 25.4 ± 0.5 |
| e | | 0.1%, 15 | 6%, 90 | ∼100 | 14.3 ± 0.6 |
| f | 100 μm | 1%, 10 | 3%, 60 | ∼60 | 14.9 ± 0.2 |
| g | | 0.33%, 10 | 3%, 60 | ∼60 | 10.0 ± 0.3 |
| h | 50 μm | 1%, 4 | 3%, 20 | 15−20 | 6.9 ± 0.3 |
| i | | 0.33%, 5 | 2%, 20 | 10−20 | 5.6 ± 0.4 |

film of eyes and the ability of mucoadhesive materials to prolong their residence time on the mucosa, thus increasing the bioavailability of the administered drug.[4,8]

The typical mucus layer is a highly hydrated non-Newtonian, viscoelastic system composed of a 3D network of randomly entangled high molecular weight glycoproteins named mucins (2−5 wt %),[6,8] with an average thickness of 3−5 μm on the cornea.[9,10] Understanding the interactions between polymeric mucoadhesive materials and the mucosa is critical for the rational development of mucoadhesive drug delivery systems.[8] Mucoadhesive polymers interact with mucins via a variety of well-studied mechanisms, including electrostatic interactions, hydrogen bonding, van der Waals forces, and polymer chain interdiffusion.[11,12] These polymers are typically coated/grafted onto the surfaces of drug-loaded microparticles, and two major factors (i.e., surface chemistry/charge and microparticle size) can be modulated to enhance their adhesion to the mucosa. As far as the first factor is concerned, polysaccharides are extensively studied natural polymers in drug delivery applications because of their general stability, low toxicity, hydrophilicity, biodegradability,[13] and the presence of reactive functional groups (e.g., amine groups) that promote mucoadhesion.[11] Chitosan, a polysaccharide obtained from chitin, has emerged as an important mucoadhesive biomaterial[14] that is extensively utilized in ocular drug delivery,[15] especially as a coating material for micro and nanoparticles (MPs and NPs)[16−20] in administration routes including oral, nasal, and pulmonary.[8] The mucoadhesive properties of chitosan are due to the formation of secondary chemical bonds such as hydrogen bonds, hydrophobic interactions, and more importantly, electrostatic interactions[14,21] between the oppositely changed chitosan and mucins. The dimension of MPs and NPs is a second crucial modulator of their mucoadhesion behavior. The high surface area-to-volume ratio of NPs makes them very attractive for mucoadhesive formulations because of the high interfacial areas available for the establishment of adhesive bonds.[8] In general, submicron nanoparticles are able to diffuse into the mucus layer, where their translocation depends on multiple factors, particularly their adhesive properties and size. Diffusion of adhesive NPs is slower than nonadhesive ones because of the mucoadhesion interactions, and consequently, they are primarily retained in the periphery of the mucus layer.[18] Studies using human cervical mucus found that because of the heterogeneity of the mucus mesh, larger particles (e.g., 200−500 nm) can diffuse faster than smaller particles (100 nm or less), which can access tortuous and dead-end channels.[22] However, in tighter mucus mesh, diffusion of larger nanoparticles is substantially reduced relative to smaller nanoparticles.[23] While smaller size is an overall advantage for mucoadhesion, it poses challenges for sustained drug delivery. NP formulations are typically characterized by burst release properties, which may not be suitable for a sustained release formulation.[24,25] On the other hand, larger particles in the micrometric range (MPs) potentially enable sustained drug delivery, yet face the opposite challenge of weaker mucoadhesion since they are incapable of fully embedding into the mucosa.[8] As a result, MPs are typically exposed to the harsh hydrodynamic environment of the eye and experience large shear rates approaching 28 500 $s^{-1}$ due to reflex blinking,[26] thereby accelerating their clearance from the eye surface. There have been some studies using flow chambers to examine effect of diameter on adhesion of MPs, but these have been limited to shear rates far lower than their physiological counterparts in the eye.[27]

From the perspective of rational design, the question of what optimal particle size range allows sustained drug delivery while retaining strong mucoadhesive behavior (and therefore enabling longer residence times in the eye) remains unresolved. This is the key issue that we examine in this paper, which we approach from the standpoint of mucoadhesion behavior. We first present experimental measurements of the adhesion of monodispersed chitosan-coated poly(lactic-*co*-glycolic acid) (PLGA) MPs in a broad size range of 15−120 μm, fabricated using microfluidic methods, to mucin-coated surfaces using atomic force microscope (AFM) force spectroscopy. We then present studies of the adhesion behavior of these PLGA MPs in mucin-coated microfluidic flow cells under physiological shear rates. Finally, we present simple scaling arguments for microparticle detachment based on the lift, drag, and friction forces experienced by the MPs and the experimentally measured adhesion forces. One of the key conclusions from our study is that MPs below a threshold diameter of ∼20 μm exhibit nearly indefinite persistence in the flow cells under physiological shear rates. This threshold dimension represents an upper limit of particle diameter for MPs that allows enhanced mucoadhesion while retaining the sustained delivery properties enabled by larger particle dimensions. Our findings therefore address the open question articulated above and pave the way for the rational design of MP-based ocular drug delivery systems to improve the bioavailability of therapeutic agents.

## 2. MATERIALS AND METHODS

**2.1. Preparation of PLGA MPs.** The preparation of PLGA MPs of various diameters followed a previous procedure with minor modifications.[19] Oil-in-water (O/W) emulsions were achieved using a coaxial glass capillary microfluidic setup (Figure S1), which was assembled by inserting a round capillary into a square one. The surface of the round capillary was treated with an oxygen plasma (100 W) for 120 s. The aqueous continuous phase (W) (poly(vinyl alcohol) (PVA, molecular weight ∼67 kDa (Mowiol 8−88, Aldrich))



DOI: 10.1021/acsabm.8b00041
ACS Appl. Bio Mater. 2018, 1, 561−571

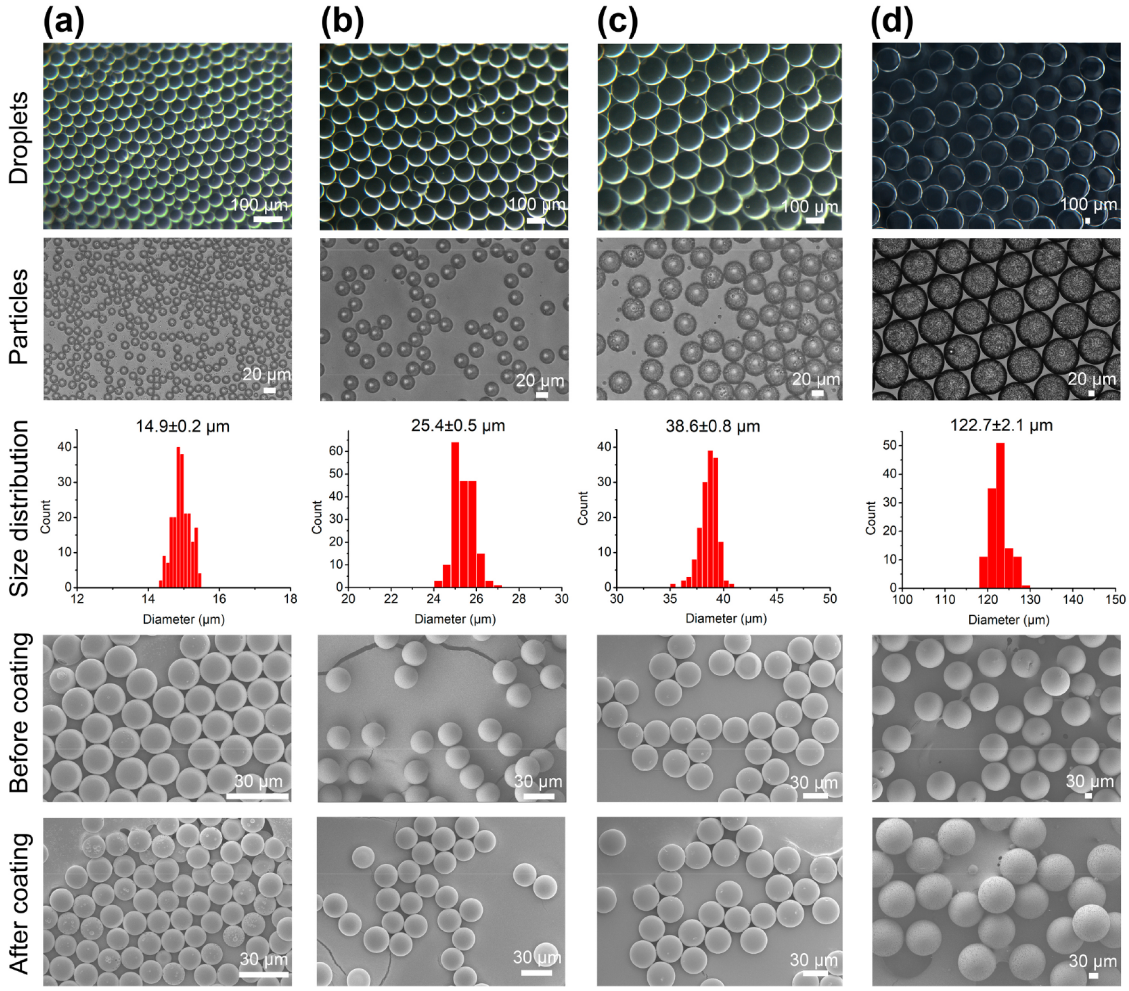


**Figure 1.** Preparation and coating of PLGA MPs by flow-focusing capillary microfluidic devices. Microscopy images of emulsion droplets and MPs, particle size distribution, SEM images of PLGA MPs prepared with 100 $\mu$m nozzle (a) and 220 $\mu$m nozzle with different PVA concentrations (b–d) before and after coating with chitosan are shown, respectively.

in water) and the dispersed phase (O) (PLGA (75:25, Sigma-Aldrich, product no. P1941, molecular weight 66–107 kDa) in dichloromethane) were infused from the two ends of the square capillary through the outer coaxial region using syringe pumps (Harvard PHD 22/2000 series). The dispersed phase was hydrodynamically focused by the continuous phase at the nozzle of the round capillary, resulting in the formation of emulsion droplets. In order to prepare different diameters of PLGA MPs, the PVA and PLGA concentrations were varied from 2% to 6%, and from 0.1% to 1% respectively, while the nozzle size and flow rate were also modulated accordingly (Table 1). Glass wells with a predispensed film of continuous phase were used for sample collection. Approximately, 300 $\mu$L of O/W emulsions was dispensed directly into the glass well with a 6 cm internal diameter to prevent droplet coalescence. Optical microscopy images of the droplets were captured using a QImaging MicroPublisher 5.0 RTV camera mounted on an Olympus SZX7 microscope. Afterward, solvent evaporation was performed at room temperature to achieve PLGA MPs of different diameters. PLGA MPs were then washed with Milli-Q water multiple times to remove PVA, dried in a vacuum drier, and stored at 4 °C for further use.

**2.2. Size Distribution and Morphology of PLGA MPs.** Size distribution and morphology of PLGA MPs were measured using microscopic image analysis and field emission scanning electron microscopy (FESEM). The size distribution was analyzed with an inverted microscope (Nikon Eclipse Ti) operated in bright field mode, whose in-built software (NIS Elements 3.22.0) was used to measure the diameters of MPs (circle by a three-point method). Each sample was comprised of at least 200 particles. The morphology of MPs was also studied by a field emission scanning electron microscope (JEOL JSM-6700F) at 5 kV accelerating voltage. All samples were coated with ~10 nm of platinum (30 mA for 70s) by sputter coating before imaging.

**2.3. Coating of PLGA MPs.** As-prepared PLGA MPs were coated in 1% (w/v) chitosan (Sigma-Aldrich, molecular weight 50–190 kDa, degree of deacetylation 75%–85%) by mixing on a rocker for 4 h and settled down by gravity. Afterward, the coated MPs were washed with water to remove the excessive chitosan and resuspended in 20 mM HEPES buffer at pH 7.4. The $\zeta$-potential of MPs in HEPES buffer before and after coating was analyzed by a Zeta-sizer (Malvern) at ~1 mg/mL MPs. Details of the method for quantification of chitosan coating on PLGA MPs, expressed as the mass of chitosan coating the PLGA MPs per mass of MPs are provided in Supporting Information.

**2.4. Preparation of Mucin-Coated Polystyrene Substrates.** Bovine submaxillary mucins (Sigma-Aldrich, product no. M3895) were purified following previous reports.[28,29] Briefly, the proteins were dissolved in Milli-Q water at 10 mg/mL and dialyzed against Milli-Q water using a Spectra/Por Float-A-Lyzer G2 dialysis membrane (100 kDa MW cutoff, Spectrum Laboratories) for 4 days with a daily change of fresh water and then lyophilized for storage. Mucin coatings were generated by incubating mucin (0.25 or 1 mg/mL) in HEPES buffer (0.02 M, pH 7.4) on the surface of polystyrene Petri dishes (Nunc, ThermoFisher Scientific) for different durations. The coated surfaces were then washed with HEPES buffer three times. For the contact angle measurement, the surfaces were further washed with


DOI: 10.1021/acsabm.8b00041
ACS Appl. Bio Mater. 2018, 1, 561–571

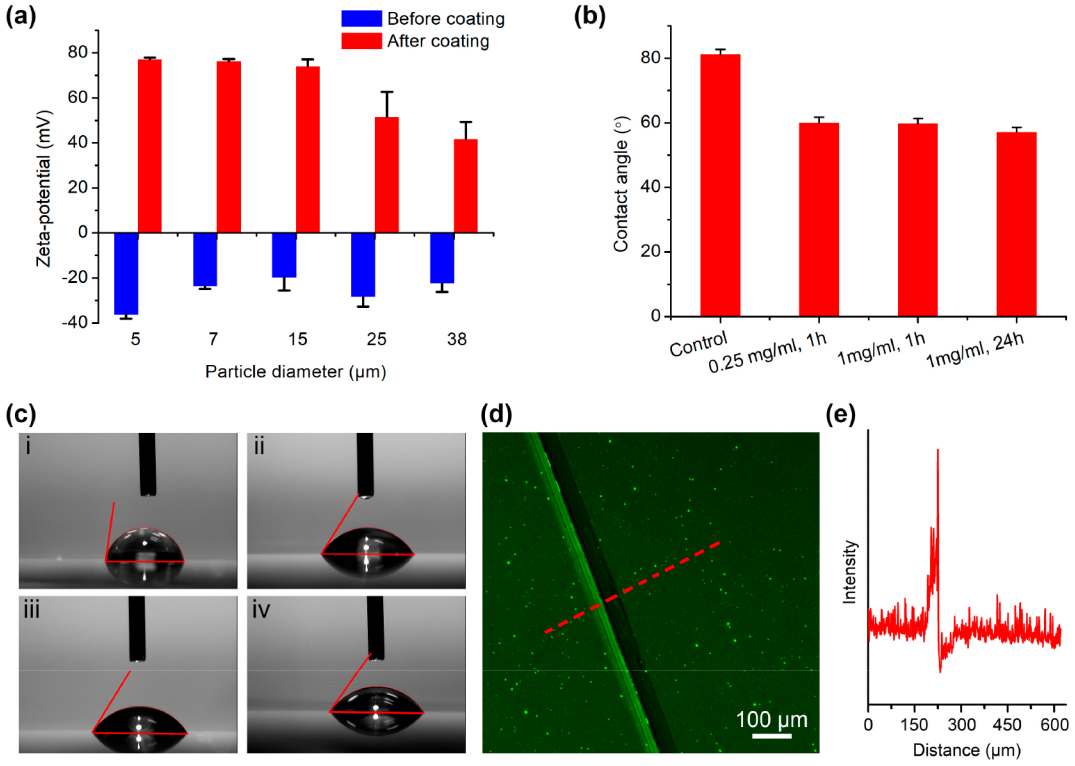


**Figure 2.** (a) $\zeta$-potential of PLGA MPs of different sizes in HEPES buffer before and after coating with chitosan. (b) Contact angle of polystyrene dishes with and without mucin coating at different protein concentrations and with different durations. (c) Representative images of contact angle measurements for polystyrene dishes with and without mucin coating. i: without coating. ii: coating with 0.25 mg/mL mucin for 1 h. iii: coating with 1 mg/mL mucin for 1 h. iv: coating with 1 mg/mL mucin for 24 h. (d) Fluorescent image of polystyrene dish coated with 5-FAM SE-labeled mucin. A scratch was made by a metal needle to display the contrast. The fluorescence intensity along the dashed line is displayed in (e).

water for three times to prevent salt crystal formation and then dried in air overnight. The contact angle of a Milli-Q water drop (1 $\mu$L) on mucin coatings was measured using a goniometer (camera-equipped VCA 2000, AST Products). The reported values were averages of five measurements at different positions of each sample. The mucin coating was also examined by fluorescence microscopy. To produce fluorescent mucins, mucins were labeled with 5-carboxyfluorescein succinimidyl ester (5-FAM SE, Bio Basic Asia Pacific) following an established procedure.[29] Refer to Supporting Information for more details of labeling, coating, and imaging.

**2.5. Mucoadhesion Study by AFM Force Spectroscopy.** The mucoadhesion forces of PLGA MPs on mucin coatings were studied by AFM force spectroscopy. All experiments were performed on a NanoWizard II AFM (JPK Instruments) installed on an inverted optical microscope (Olympus IX71) at room temperature. Colloidal probes with different sizes of PLGA MPs (15−120 $\mu$m) were glued with epoxy resin (Selleys Epoxy Fix Super Fast) onto tipless cantilevers (refer to Supporting Information for more details). The attached MPs on the cantilevers were characterized by SEM with the same method mentioned above. Force measurement on noncoated MPs were performed with softer cantilevers with a theoretical spring constant of 0.03 N/m (Arrow TL1−50 Tipless Cantilevers, NanoWorld), while those for coated MPs were done with stiffer cantilevers with a theoretical spring constant of 0.32 N/m (PNP-TR-TL-Au-50, Pyrex-Nitride AFM Probes, NanoWorld). The actual spring constant of the cantilevers were calculated by the thermal noise method.[30] The noncoated MPs were incubated in HEPES buffer (20 mM, pH 7.4) for 10−15 min, while the coated MPs incubated in 1% chitosan for 1 h, washed with water 3 times and incubated in HEPES buffer for 10−15 min as well before the force measurements. The adhesion force measurements were conducted at a constant loading force (4 nN) and constant loading rate (1 $\mu$m/s) for various particle sizes. For each particle size, force measurements were performed with various delay times upon contact ranging from 0 to 20 s on at least 20 different locations on the mucin-coated substrate with distance of more than 10 $\mu$m between locations. The reported adhesion forces are averages of minima of all force−distance curves at each condition, while the adhesion energies were obtained by calculating the work of adhesion from the measured force−distance curves (areas under curves). The rupture lengths of the curves where the MPs were completely separated from mucin coatings were also compared at different contact times.

**2.6. In Vitro Mucoadhesion Shear Test in Microfluidic Flow Cells.** We performed in vitro mucoadhesion shear tests on the noncoated and coated PLGA MPs to determine their mucoadhesive properties under conditions mimicking the physiological shear rates in tear films within human eyes.[19] A rectangular microchannel mold produced by 3D printing was used to prepare PDMS-glass microchannels (refer to Supporting Information for more details). In order to replicate the conditions of mucin coating in AFM force spectroscopy, the microchannels were coated with a polystyrene solution (~1 mg/mL, obtained by dissolving Petri dish pieces in acetone), dried overnight, and coated with mucin via the same procedure as above. The contact angle of the coated glass slide was measured as above to confirm the presence of polystyrene in the microchannels. In the following, noncoated and coated PLGA MPs at different sizes in HEPES buffer were filled into the channels respectively and allowed to settle down and immobilize in the channels for 30 min before the progressive shear test. HEPES buffer was then infused into the microchannels by syringe pumps at flow rates ranging from 0 to 80 000 $\mu$L/min, with a step-increase of flow rate of 1−5 mg/mL to investigate the particle response to increasing flow rate. Shear rate ($\dot{\gamma}$) at a specific flow rate is calculated as

$$\dot{\gamma} = [6Q/(WH^2)](1 + H/W)f(H/W) \quad (1)$$

where $Q$ is the volumetric flow rate, $W$ and $H$ are the width and height of rectangular channel, and $f(W/H)$ is an aspect-ratio dependent correction factor, which is 0.882 at $H/W$ = 0.1 used in this study.[31]



DOI: 10.1021/acsabm.8b00041
ACS Appl. Bio Mater. 2018, 1, 561−571

The number of MPs adhered to the mucin coatings at 0 shear rate is denoted by $N_0$, while the number of MPs remaining at any shear rate is denoted as $N$. The mucoadhesion ability of PLGA MPs was calculated as the percentage $N/N_0$ versus shear rate.

## 3. RESULTS AND DISCUSSION

**3.1. PLGA Microparticle Fabrication, Characterization, and Coating.** PLGA microparticles were fabricated using capillary microfluidics-based emulsion generators and solvent evaporation. A uniform stream of oil-in-water (O/W) emulsion droplets was formed in the microfluidic emulsion generator (Figure S2) and collected in a glass well with a predispensed film of PVA solution. The droplets shrank upon solvent evaporation at room temperature until the formation of spherical PLGA MPs (Figure 1). Slow evaporation of solvent from the droplets allows complete annealing of the polymer, in turn leading to high stability and slow particle degradation rates.[32] Generally, the final particle sizes were ∼25% of the original droplet sizes at a PLGA concentration of 1 wt %. In order to achieve PLGA particles of widely varying sizes, several parameters in the process of droplet preparation and particle formation were modulated, including the nozzle size of microfluidic device, PVA concentration, flow rates of both phases, as well as the PLGA concentration (Table 1). Briefly, smaller nozzle, lower PLGA concentration, relatively higher PVA concentration and high ratio of flow rates of W/O phases resulted in smaller droplets and hence smaller MPs. Thus, we were able to tune the particle size over a wide range from ∼5 μm to ∼120 μm (Figure 1 and Figure S3), a much broader range of diameters than what has been reported previously for this technique. Equally importantly, taking advantage of the superior control over droplet size enabled by microfluidics, the standard deviation (SD) of resultant PLGA particles was always less than 5% and even less than 2% at relatively larger particle size (Figure 1 and Figure S3), in agreement with our previous work.[19] In contrast, conventional techniques of preparing PLGA MPs including sonication, spray drying, and batch emulsification usually generate polydisperse particles with a broad size distribution,[33] which also suffer from batch-to-batch variations.[34] The morphology and particle sizes of the resultant PLGA MPs were also analyzed by FESEM, which confirmed the spherical shape. Compared to the observation under an optical microscope, the mean diameters of PLGA MPs were marginally smaller under FESEM, probably due to swelling of PLGA polymer chains as a result of relatively hydrophilic 25% glycolic acid units[35] in the former condition.

To enable mucoadhesion, the PLGA MPs were coated with 1% (w/v) chitosan in 0.5% acetic acid and washed with water. A wide range of polymers, including natural ones such as alginate, chitosan, and hyaluronic acid and synthetic alternatives like poly(ethylene glycol) (PEG), poly(acrylic acid), and poly(vinyl amine), have been investigated in mucoadhesion studies.[8] Chitosan was chosen in this study because of its outstanding mucoadhesion performance. SEM images revealed that there was no significant change in particle diameter and morphology after chitosan coating (Figure 1 and Figure S3), which was consistent with previous studies.[36,37] On the other hand, as expected, we observed a large change of ζ-potential after the coating (Figure 2a). Uncoated particles had a ζ-potential of around −20 mV due to the presence of carboxyl groups at the end of polymer chains. After coating there was a shift to positive ζ-potential greater than 40 mV, which confirmed the presence of chitosan on particle surfaces. Moreover, ζ-potential increased inversely with particle size, from ∼40 mV at 38 μm to almost 80 mV below 15 μm in particle diameter. Using the ninhydrin method,[38] we quantified the chitosan coating on PLGA MPs, which is expressed as μg chitosan per mg of MPs. The coating on 15 μm MPs was 1.84 μg (chitosan)/mg (MPs), while that for 25 and 38 μm MPs was 1.16 and 0.69 μg/mg respectively (Figure S4); this is an expected trend given the higher surface-to-volume ratios of smaller MPs. Furthermore, the measured chitosan coating ratio between 38, 25, and 15 μm MPs was 1:1.68:2.67, slightly higher than their relative surface-to-volume ratios (1:1.52:2.53), suggesting a relatively denser chitosan coating on smaller MPs. This trend is also in agreement with the higher ζ-potential of 15 μm MPs compared with their larger counterparts (Figure 2a).

**3.2. Fabrication of Mucin-Coated Substrates.** To achieve an in vitro surface that is able to mimic the natural mucus surface for the mucoadhesion analysis of PLGA MPs, we generated mucin coatings by incubating 1 mg/mL mucin solution on a polystyrene surface for 24 h.[28,29] Adsorption of mucin to polystyrene is presumably driven by hydrophobic interactions between the surface and the mucin protein core.[39,40] Contact angle measurement was used to verify the coating of mucin on polystyrene surfaces. Compared with uncoated hydrophobic surfaces, the coated surfaces exhibit decreases in contact angle by more than 20 degrees (Figure 2b,c), which was comparable to previous reports.[29] According to the literature, the thickness of coating in hydrated conditions is around 60−70 nm.[29] Coating at lower concentration (0.25 mg/mL) and shorter duration (1 h) showed a similar decrease in contact angle, suggesting a robust mucin coating procedure. Moreover, these results are in line with a previous study,[28] where the coating of mucin on polystyrene surfaces tended to saturate within 1 h in terms of coating thickness. That being said, given the marginally lower contact angle for the surface with 24 h coating, this condition was selected for all subsequent studies of mucoadhesion to keep the coating thickness consistent. In addition, we monitored each batch of mucin coating by the measurement of contact angle, which indeed displayed good consistency among batches. The mucin coating was also found to be robust and reusable because the contact angle did not change after the dehydration and rehydration of coating surfaces (Figure S5). Finally, in order to further visualize the coating of mucin on polystyrene surfaces, the protein was labeled by 5-FAM SE, coated on the PS surface following the same procedure as above and analyzed by fluorescence microscopy. Fluorescent imaging revealed a relatively homogeneous coating of proteins on the surface except a few highly fluorescent spots, which might result from protein aggregation (Figure 2d). Furthermore, a scratch in the image showed a significant contrast of fluorescence intensities (Figure 2e). Similarly, a substantial difference of fluorescence intensities was also found at the boundary regions of mucin coatings (Figure S6), agreeing with the contrast found in the scratch. Taken together, these data validated the presence of a robust mucin coating that was used in the following mucoadhesion studies.

**3.3. AFM Force Spectroscopy.** AFM has been widely utilized to investigate bio- and mucoadhesion.[41,42] Compared with other methods such as rheological[43] and tensile force measurements,[44] particle counting/imaging,[45] flow chamber analysis,[46] and optical tweezers,[18] AFM provides better insight into how two surfaces adhere to and separate from each other,


DOI: 10.1021/acsabm.8b00041
ACS Appl. Bio Mater. 2018, 1, 561−571

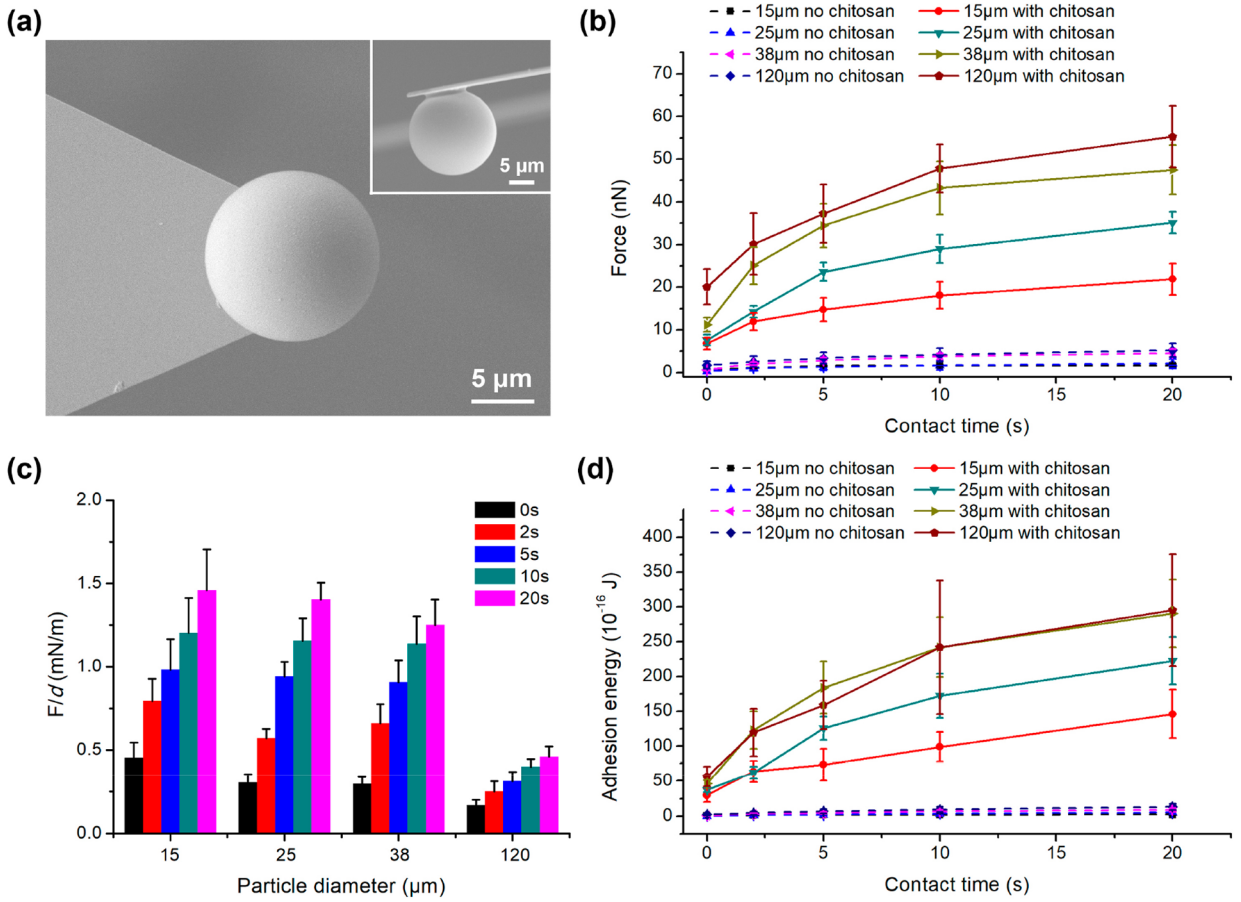


**Figure 3.** (a) SEM images of 15 $\mu$m PLGA MP attached to the AFM cantilever. The inset shows the side view of the cantilever. (b) Adhesion forces as a function of contact time by AFM studies between mucin coatings on the polystyrene dishes and PLGA MPs at different sizes with or without chitosan coating. (c) Adhesion forces between mucin coating and chitosan coated PLGA MPs normalized by particles diameter *d*. (d) Adhesion energy as a function of contact time between mucin coatings on the polystyrene dishes and PLGA MPs at different sizes with or without chitosan coating.

from the measured force−distance curves.[47] It has previously been used in adhesion force measurements between mucin surfaces and polymeric or glass particles coated with a variety of mucoadhesive polymers including polyether modified poly(acrylic acid),[42] PEG,[48] and biomimetic nanowire coatings.[49] However, mucoadhesion between chitosan-coated particles and mucin-coated substrates has been seldom studied before, with the closest study being a report on adhesion measurements between mucin and a PLGA modified AFM probe coated with chitosan, which lacked the tunability of probe size.[50] In our study, we modified AFM probes by attaching the PLGA MPs directly onto tipless probes with epoxy glue (Figure 3a). In order to avoid the possibility of contaminating the particle with glue,[50] the probe was touched on clean surfaces a few times before approaching the MP (Figure 3a inset). A key advantage of this method is it allowed the attachment of particles of customized diameters. For parity across experiments, all MPs were brought into contact with the mucin coating with the same loading force and the buffer condition was 20 mM HEPES at pH 7.4, given that the mucoadhesive performance of chitosan is higher at neutral or slightly alkaline condition as in the human tear film.[51]

Figure 3b,d present measurements of adhesion forces and energies as a function of contact time for coated and uncoated particles of various sizes, and Figure 3c presents adhesion forces normalized by particle diameter *d*. Larger MPs clearly exhibited higher adhesion forces. We observed a significant spontaneous adhesion force at 0 s contact (Figure 3b), arising from attractive electrostatic interactions between cationic chitosan molecules and the anionic mucin coating.[6,11] The adhesion force for all particle sizes rapidly grew with contact time and saturated beyond 10 s. In addition to particle size, it has been reported that surface roughness of particles might also play a role in mucoadhesion.[52] In our studies, we expect the surface roughness of PLGA MPs investigated in AFM studies and shear testing to be constant across the different particle sizes due to the consistency of the preparation and coating procedures. Indeed, all particle surfaces were observed to be smooth under SEM imaging (Figure 1, SEM images before coating). The thickness of chitosan coating in water has been reported to lie in the ∼100 nm range.[36] Moreover, the coating is flexible in solution due to its gel-like structure. Thus, we anticipate the chitosan coating to be able to mask particle surface roughness at the sub-100 nm length scales, which are inaccessible to direct observation under the SEM.

Figure 4 shows representative retraction curves of PLGA MPs from the mucin coating with different contact durations in the force−distance mode, normalized by the particle diameter. Generally, all curves exhibited characteristic sawtooth profiles during the separation of a particle from the surface (the collection of experimentally measured curves for 15 $\mu$m MP at various contact times is provided in Figure S7),


DOI: 10.1021/acsabm.8b00041
ACS Appl. Bio Mater. 2018, 1, 561−571

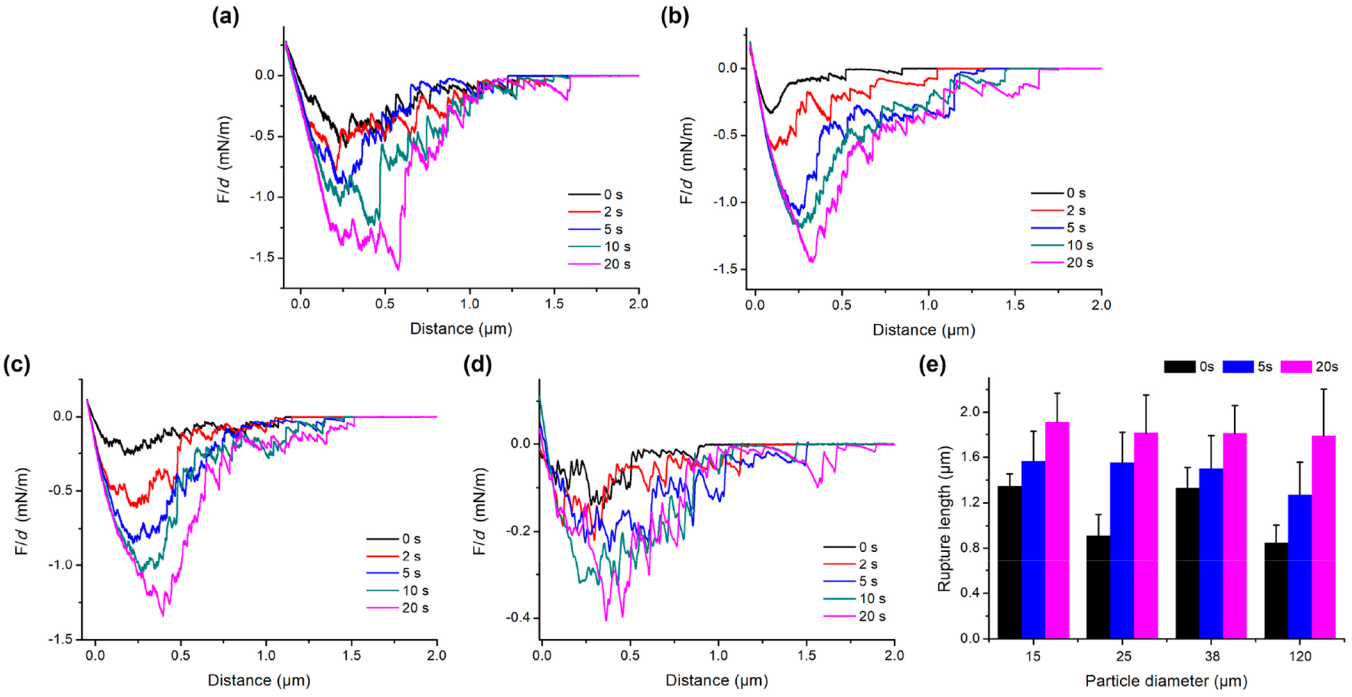


**Figure 4.** Normalized force−distance curves of PLGA MPs with different sizes from 15 (a), 25 (b) to 38 (c) and 120 $\mu$m (d) on mucin coatings at different contact times by AFM study. (e) Rupture lengths between PLGA MPs and mucin coatings in HEPES buffer.

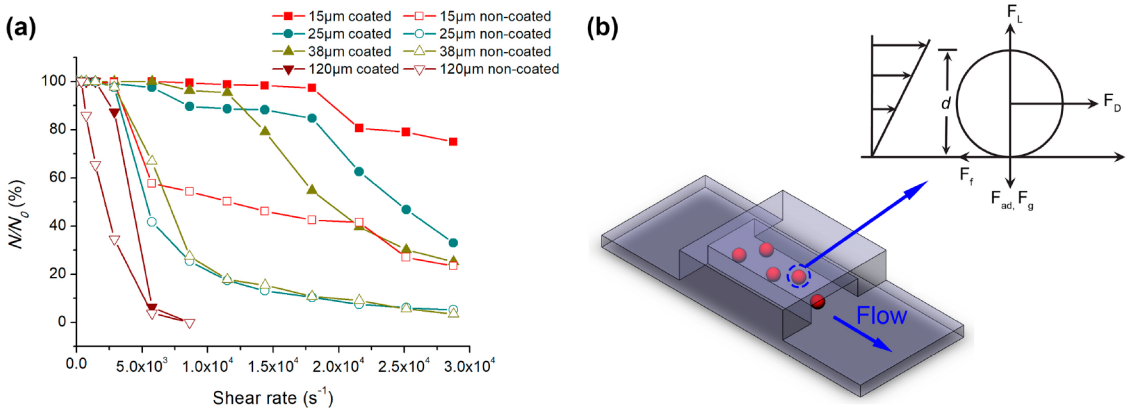


**Figure 5.** (a) Retention capability of PLGA MPs with different sizes in mucin coated PDMS channels against increasing shear rate. (b) Schematic diagram of shear test of MPs. The inset shows forces experienced by a mucoadhesive PLGA MP attached to a mucin surface.

which was in line with previous adhesion studies between mucin and chitosan,[53] and between other polymers or particles.[47,54] As proposed by previous reports, each sawtooth in the profile may be attributed to the breakage of interactions between mucin and chitosan molecules (either hydrogen bonding or electrostatic interactions).[14,21] The sequence of sawtooths in the measured force−distance curves suggests a stepwise disruption of mucin−chitosan interactions during the particle retraction, resulting in a rupture length (defined as the length from the contact point to the rupture point where the adhesion force becomes zero)[47] that is much longer than the thickness of either the mucin or chitosan coating on both surfaces. This is likely due to the stepwise stretching and detachment of long entangled polymer chains of chitosan and mucin (~7000 kDa and up to micrometers in length).[8,53] Furthermore, since stretching single molecules usually requires forces on the order of a few hundred pN,[55] the measured magnitudes of the sawtooth minima in $\mu$N range implied that each sawtooth could be attributed to stretching and detachment of multiple mucin and chitosan molecules involved in the mucoadhesion. Moreover, we observed a significant increase in rupture length with incubation time, implying consolidation and strengthening of mucoadhesion contacts (Figure 4e) via polymer chain interpenetration and secondary bonding. This increase in rupture length was also accompanied by an increase in the number of sawtooths in the curves (Figure 4a−d).

**3.4. Particle Detachment Studies in Microfluidic Flow Cells.** Next, we performed in vitro particle detachment tests under shear stress in a microfluidic flow cell. Coated and uncoated PLGA microparticles were subjected to progressive shearing to determine their mucoadhesive strength in a slit-like PDMS-based channel (Figure 5b and Figure S8). In order to minimize the influence of channel walls on the flow rate, we used a high aspect ratio of channel width to height of 10:1.[46] To maintain parity with the preceding AFM studies, we coated the glass substrate with a thin layer of polystyrene prior to the



DOI: 10.1021/acsabm.8b00041
ACS Appl. Bio Mater. 2018, 1, 561−571

mucin coating. After coating, the contact angle increased from ∼30° to >90° (Figure S9), verifying the presence of polystyrene on the glass. The coated and uncoated PLGA MPs with different diameters were deposited in the channels and allowed to settle for 30 min before starting the flow. To mimic the shear experienced in eye movements including blinking, saccade, smooth pursuit, microsaccades and tremors,[26] the shear rate was progressively increased to ∼28,750 $s^{-1}$, which is comparable to the maximum shear rate during eye blinking.[26] Agreeing with the AFM force measurements, the coating of MPs endowed them with significantly higher ability to withstand shear stress (Figure 5a and Figure S10), and smaller particles adhered better than larger ones: more than 70% of the 15 $\mu$m MPs were retained under the highest physiologically relevant shear rate, while larger MPs were more prone to detach. In the section below, we discuss the connection between these measurements and the AFM measurements of the previous section in more detail. In particular, we highlight a phenomenon of importance in rational particle design—the existence of a *threshold* particle diameter below which coated MPs exhibit indefinite adhesion at a given shear rate.

**3.5. Connecting AFM Measurements to Shear Detachment Studies: Effect of Particle Size.** Figure 5b (inset) schematically depicts a chitosan-coated PLGA MP of diameter $d$ adhered to the mucin surface with adhesion force $F_{ad}$, and experiencing an additional gravitational force $F_g$. The MP also experiences drag ($F_D$) and lift ($F_L$) forces in linear shear flows.[56,57] Particle detachment can be initiated via direct lift-off, when $F_L$ exceeds $F_{ad}$ and $F_g$, or by sliding of a MP from the surface when $F_D$ exceeds the frictional force $F_f$ experienced during horizontal motion along the mucin-coated surface. From previous studies on the hydrodynamics of wall-attached particles in linear shear flows, it is known that $F_D$ scales as $\sim d^2$,[56] while $F_L$ scales as $\sim d^{3.12}$.[57] These forces are also linear and nonlinear functions of the shear rate, respectively. $F_g$ is negligible under all conditions in our studies. As a first approximation, if frictional force $F_f$ corresponds to classical sliding friction, then it is simply proportional to the net vertical force ($F_{ad} - F_L$). However, the proportionality constant (i.e., the coefficient of sliding friction,) involves considerable uncertainty and is not amenable to a simple analysis. Finally, the adhesion force ($F_{ad}$) of MPs can be fitted as a function of particle diameter; in the smaller size range (<38 $\mu$m in diameter), $F_{ad}$ scales nearly linearly with $d$ (Figure S11).

Now, equating $F_L$ to $F_{ad}$ yields a *threshold* particle diameter at a given shear rate, at which lift is balanced by adhesion. Below this threshold size, particles will remain adhered to the surface at that shear rate. Likewise, equating $F_D$ to $F_f$ yields another threshold diameter for the force balance in the horizontal direction. The threshold size observed in measurements corresponds to the smaller of these two sizes. This simple analysis sheds light on the measurements of Figure 5a. First, our measurements do show this threshold behavior, in that the 15 $\mu$m MPs were indefinitely retained in the microfluidic flow cell, while larger particle sizes are detached from the mucin-coated walls at progressively increased shear rates. Moreover, during the shear detachment experiments, we observed very few sliding MPs. Instead, most of particles remained in their original positions until detachment occurred in quick events by direct lift-off from the substrate (Figure S10). Interestingly, a simple calculation of threshold particle diameter at the maximum shear rate (28,750 $s^{-1}$) due to lift forces yields an estimate of ∼21 $\mu$m (Supporting Information), which is in reasonable agreement with our particle detachment experiments.

Finally, it is important to note that the measured threshold corresponds to a MP diameter in the ∼20 $\mu$m range, which has important ramifications on formulation design. With this insight at hand, it is now possible to envision and design particle-based topical drug-delivery systems in the 20 $\mu$m range that satisfy two opposing constraints—enhanced mucoadhesion under shear, which is favored at *smaller* particle diameters, and sustained drug delivery with tailored release constants, which is favored by *larger* particle diameters. In other words, mucoadhesion performance "saturates" below a particle diameter threshold in the 20 $\mu$m range. Our results suggest that indefinitely decreasing the particle diameter below this threshold will show the *same* mucoadhesion performance *in vivo* but markedly *different* drug release performance, tending toward rapid burst release profiles, which may or may not be desirable depending on the intended application. Concerning tolerability of MP-based topical formulations, it is possible that eye discomfort increases with MP size. However, there is no clear upper bound of particle size beyond which MPs are considered to cause discomfort;[58] it has been reported that particle sizes less than 10 $\mu$m can minimize eye irritation.[59] Furthermore, particle shape and concentration are also key factors that make it difficult to define a sharp limiting size that marks the onset of eye irritation or discomfort. An *in vivo* study found no extraordinary tearing in rabbits treated with 0.1% dexamethasone suspensions with average sizes from 5 to 22 $\mu$m, and containing MPs larger than 30 $\mu$m.[58]

As mentioned above, ours is the first study to conduct force measurements on chitosan-coated microparticles to investigate the effect of microparticle size on mucoadhesion. The closest related work reported force measurements between a mucin film and a PLGA-modified AFM probe coated with chitosan but did not investigate the effect of probe size. Thus, it is difficult to make a direct comparison of our study with other published results of mucin adhesion with chitosan coated surfaces. That being said, we anticipate that our conclusions could be extended to a range of mucoadhesive polymers that exhibit similar mechanisms of adhesion, that is, rapid electrostatic interactions reinforced by secondary interactions (e.g., hydrogen bonds and polymer chain interdiffusion),[14] such as hyaluronic acid and ploy(vinyl amine),[8] and to chitosan-coated/conjugated particles composed of other substrates including alginate,[60] dextran,[61] and liposomes.[62] In addition, given that the mucus layer in eyes is subjected to the harshest in vivo shear stress conditions compared with mucosa in other tissues such as the gastrointestinal and respiratory tracts, our study will also be useful for the design of mucoadhesive drug-delivery systems for those tissues.

## 4. CONCLUSIONS

In summary, monodisperse chitosan-coated PLGA MPs with controllable diameters from 5 to 120 $\mu$m have been fabricated for ocular drug delivery applications. We have presented the first measurements of adhesion of chitosan-coated MPs to mucin-coated substrates by AFM force spectroscopy. The MPs displayed strong instantaneous adhesion to the mucin-coated surfaces, with characteristic sawtooth-like force–distance curves and particle-diameter- and contact-time-dependent rupture lengths, adhesion forces, and energies. Particle detachment tests under shear stress were conducted in a


DOI: 10.1021/acsabm.8b00041
ACS Appl. Bio Mater. 2018, 1, 561–571

microfluidic flow cell to examine their mucoadhesion under in vitro conditions that closely mimic the in vivo hydrodynamic environment. It was found that more than 70% of the 15 $\mu$m MPs were retained under the highest physiologically relevant shear, while larger MPs were easier to detach. A simple analysis of forces experienced by the MPs reveals the existence of a threshold size at a given shear rate, below which particles remain indefinitely adhered to the surfaces, highlighting the key fact that mucoadhesion performance saturates below a threshold in particle diameter. These findings provide valuable guidance for the rational development of mucoadhesive microparticulate ocular drug delivery systems that are capable of withstanding harsh ocular environments and prolonging their residence on corneal surfaces, thereby enhancing the bioavailability of drugs topically applied to eyes. They also shed light on the design of drug delivery systems to other mucosae-related organs, given the universal presence of mucin proteins in a variety of tissues including buccal, nasal, lung, gastric, and intestinal mucosae.[8]

## ■ ASSOCIATED CONTENT

### Supporting Information

The Supporting Information is available free of charge on the ACS Publications website at DOI: 10.1021/acsabm.8b00041.

Additional experimental details; schematic figure of the preparation of monodisperse PLGA MPs by a capillary microfluidic device; microscopic image of the PLGA droplet formation by microfluidic technique; preparation and coating of smaller PLGA MPs with a 50 $\mu$m nozzle; quantification of chitosan coating on PLGA MPs; comparison of contact angle between fresh mucin and rehydrated mucin coating; fluorescence image of 5-FAM SE labeled mucin coatings; force−distance curves of 15 $\mu$m PLGA MPs by AFM force spectroscopy; image of the PDMS-glass microchannel for particle detachment study; contact angle of glass and polystyrene-coated glass; retention of 15 $\mu$m PLGA MPs on the mucin coating in the shear test at different flow rates (shear rates); fitting of adhesion force against particles size for PLGA MPs; the calculation of threshold particle diameter by equating lift force to adhesion force (PDF)

## ■ AUTHOR INFORMATION


### Corresponding Authors

*E-mail: saifkhan@nus.edu.sg.
*E-mail: pdoyle@mit.edu.

### ORCID

Dawei Ding: 0000-0002-9713-646X
Ambika Somasundar: 0000-0001-8545-0323
Patrick S. Doyle: 0000-0003-2147-9172


### Notes

The authors declare no competing financial interest.

## ■ ACKNOWLEDGMENTS

This project was supported by the National Research Foundation of Singapore through an Intra-CREATE grant and SMART center's BioSyM IRG research programme. We also express our thanks to Ms. Lu Zheng (Department of Chemical and Biolomolecular Engineering, National University of Singapore), Dr. Fang Kong and Ms. Bena Lim (Infectious Diseases (ID) IRG, SMART) for their supportive technical suggestions and help.

## ■ REFERENCES


(1) Pascolini, D.; Mariotti, S. P. Global Estimates of Visual Impairment: 2010. *Br. J. Ophthalmol.* **2012**, *96*, 614−618.
(2) Ali, Y.; Lehmussaari, K. Industrial Perspective in Ocular Drug Delivery. *Adv. Drug Delivery Rev.* **2006**, *58*, 1258−1268.
(3) Quigley, H. A.; Broman, A. T. The Number of People with Glaucoma Worldwide in 2010 and 2020. *Br. J. Ophthalmol.* **2006**, *90*, 262−267.
(4) Le Bourlais, C.; Acar, L.; Zia, H.; Sado, P. A.; Needham, T.; Leverge, R. Ophthalmic Drug Delivery Systems-Recent Advances. *Prog. Retinal Eye Res.* **1998**, *17*, 33−58.
(5) Taylor, S. A.; Galbraith, S. M.; Mills, R. P. Causes of Non-Compliance with Drug Regimens in Glaucoma Patients: a Qualitative Study. *J. Ocul. Pharmacol. Ther.* **2002**, *18*, 401−409.
(6) Ludwig, A. The Use of Mucoadhesive Polymers in Ocular Drug Delivery. *Adv. Drug Delivery Rev.* **2005**, *57*, 1595−1639.
(7) Gaudana, R.; Ananthula, H. K.; Parenky, A.; Mitra, A. K. Ocular Drug Delivery. *AAPS J.* **2010**, *12*, 348−60.
(8) Sosnik, A.; das Neves, J.; Sarmento, B. Mucoadhesive Polymers in the Design of Nano-Drug Delivery Systems for Administration by Non-Parenteral Routes: A review. *Prog. Polym. Sci.* **2014**, *39*, 2030−2075.
(9) Schmoll, T.; Unterhuber, A.; Kolbitsch, C.; Le, T.; Stingl, A.; Leitgeb, R. Precise Thickness Measurements of Bowman's Layer, Epithelium, and Tear Film. *Optom. Vis. Sci.* **2012**, *89*, E795−802.
(10) Werkmeister, R. M.; Alex, A.; Kaya, S.; Unterhuber, A.; Hofer, B.; Riedl, J.; Bronhagl, M.; Vietauer, M.; Schmidl, D.; Schmoll, T.; Garhofer, G.; Drexler, W.; Leitgeb, R. A.; Groeschl, M.; Schmetterer, L. Measurement of Tear Film Thickness Using Ultrahigh-Resolution Optical Coherence Tomography. *Invest. Ophthalmol. Visual Sci.* **2013**, *54*, 5578−5583.
(11) Smart, J. D. The Basics and Underlying Mechanisms of Mucoadhesion. *Adv. Drug Delivery Rev.* **2005**, *57*, 1556−1568.
(12) Shaikh, R.; Raj Singh, T. R.; Garland, M. J.; Woolfson, A. D.; Donnelly, R. F. Mucoadhesive Drug Delivery Systems. *J. Pharm. BioAllied Sci.* **2011**, *3*, 89−100.
(13) Liu, Z.; Jiao, Y.; Wang, Y.; Zhou, C.; Zhang, Z. Polysaccharides-Based Nanoparticles as Drug Delivery Systems. *Adv. Drug Delivery Rev.* **2008**, *60*, 1650−1662.
(14) Sogias, I. A.; Williams, A. C.; Khutoryanskiy, V. V. Why Is Chitosan Mucoadhesive? *Biomacromolecules* **2008**, *9*, 1837−1842.
(15) de la Fuente, M.; Raviña, M.; Paolicelli, P.; Sanchez, A.; Seijo, B.; Alonso, M. J. Chitosan-Based Nanostructures: A Delivery Platform for Ocular Therapeutics. *Adv. Drug Delivery Rev.* **2010**, *62*, 100−117.
(16) Werle, M.; Takeuchi, H. Chitosan-aprotinin Coated Liposomes for Oral Peptide Delivery: Development, Characterisation and in vivo Evaluation. *Int. J. Pharm.* **2009**, *370*, 26−32.
(17) Chakravarthi, S. S.; Robinson, D. H. Enhanced Cellular Association of Paclitaxel Delivered in Chitosan-PLGA Particles. *Int. J. Pharm.* **2011**, *409*, 111−120.
(18) Kirch, J.; Schneider, A.; Abou, B.; Hopf, A.; Schaefer, U. F.; Schneider, M.; Schall, C.; Wagner, C.; Lehr, C. M. Optical Tweezers Reveal Relationship between Microstructure and Nanoparticle Penetration of Pulmonary Mucus. *Proc. Natl. Acad. Sci. U. S. A.* **2012**, *109*, 18355−18360.
(19) Leon, R. A. L.; Somasundar, A.; Badruddoza, A. Z. M.; Khan, S. A. Microfluidic Fabrication of Multi-Drug-Loaded Polymeric Microparticles for Topical Glaucoma Therapy. *Part. Part. Syst. Charact.* **2015**, *32*, 567−572.
(20) Seyfoddin, A.; Sherwin, T.; Patel, D. V.; McGhee, C. N.; Rupenthal, I. D.; Taylor, J. A.; Al-Kassas, R. Ex vivo and In vivo Evaluation of Chitosan Coated Nanostructured Lipid Carriers for Ocular Delivery of Acyclovir. *Curr. Drug Delivery* **2016**, *13*, 923−934.
(21) Silva, C. A.; Nobre, T. M.; Pavinatto, F. J.; Oliveira, O. N. Interaction of Chitosan and Mucin in a Biomembrane Model Environment. *J. Colloid Interface Sci.* **2012**, *376*, 289−295.

(22) Lai, S. K.; O'Hanlon, D. E.; Harrold, S.; Man, S. T.; Wang, Y.-Y.; Cone, R.; Hanes, J. Rapid Transport of Large Polymeric Nanoparticles in Fresh Undiluted Human Mucus. *Proc. Natl. Acad. Sci. U. S. A.* **2007**, *104*, 1482−1487.
(23) das Neves, J.; Bahia, M. F.; Amiji, M. M.; Sarmento, B. Mucoadhesive Nanomedicines: Characterization and Modulation of Mucoadhesion at the Nanoscale. *Expert Opin. Drug Delivery* **2011**, *8*, 1085−1104.
(24) Couvreur, P. Nanoparticles in Drug Delivery: Past, Present and Future. *Adv. Drug Delivery Rev.* **2013**, *65*, 21−23.
(25) Agnihotri, S. A.; Mallikarjuna, N. N.; Aminabhavi, T. M. Recent Advances on Chitosan-Based Micro- and Nanoparticles in Drug Delivery. *J. Controlled Release* **2004**, *100*, 5−28.
(26) Purves, D. *Neuroscience*; Oxford University Press: London, 2012.
(27) Patil, V. R. S.; Campbell, C. J.; Yun, Y. H.; Slack, S. M.; Goetz, D. J. Particle Diameter Influences Adhesion under Flow. *Biophys. J.* **2001**, *80*, 1733−1743.
(28) Crouzier, T.; Jang, H.; Ahn, J.; Stocker, R.; Ribbeck, K. Cell Patterning with Mucin Biopolymers. *Biomacromolecules* **2013**, *14*, 3010−3016.
(29) Co, J. Y.; Crouzier, T.; Ribbeck, K. Probing the Role of Mucin-Bound Glycans in Bacterial Repulsion by Mucin Coatings. *Adv. Mater. Interfaces* **2015**, *2*, 1500179.
(30) Haugstad, K.; Håti, A.; Nordgård, C.; Adl, P.; Maurstad, G.; Sletmoen, M.; Draget, K.; Dias, R.; Stokke, B. Direct Determination of Chitosan−Mucin Interactions Using a Single-Molecule Strategy: Comparison to Alginate-Mucin Interactions. *Polymers* **2015**, *7*, 161−185.
(31) Son, Y. Determination of Shear Viscosity and Shear Rate from Pressure Drop and Flow Rate Relationship in a Rectangular Channel. *Polymer* **2007**, *48*, 632−637.
(32) Allison, S. D. Analysis of Initial Burst in PLGA Microparticles. *Expert Opin. Drug Delivery* **2008**, *5*, 615−628.
(33) Mainardes, R. M.; Evangelista, R. C. PLGA Nanoparticles Containing Praziquantel: Effect of Formulation Variables on Size Distribution. *Int. J. Pharm.* **2005**, *290*, 137−144.
(34) Xu, Q.; Hashimoto, M.; Dang, T. T.; Hoare, T.; Kohane, D. S.; Whitesides, G. M.; Langer, R.; Anderson, D. G. Preparation of Monodisperse Biodegradable Polymer Microparticles Using a Microfluidic Flow-Focusing Device for Controlled Drug Delivery. *Small* **2009**, *5*, 1575−1581.
(35) Makadia, H. K.; Siegel, S. J. Poly Lactic-co-Glycolic Acid (PLGA) as Biodegradable Controlled Drug Delivery Carrier. *Polymers* **2011**, *3*, 1377−1397.
(36) De Campos, A. M.; Sanchez, A.; Gref, R.; Calvo, P.; Alonso, M. J. The effect of a PEG versus a Chitosan Coating on the Interaction of Drug Colloidal Carriers with the Ocular Mucosa. *Eur. J. Pharm. Sci.* **2003**, *20*, 73−81.
(37) Chronopoulou, L.; Massimi, M.; Giardi, M. F.; Cametti, C.; Devirgiliis, L. C.; Dentini, M.; Palocci, C. Chitosan-Coated PLGA Nanoparticles: a Sustained Drug Release Strategy for Cell Cultures. *Colloids Surf., B* **2013**, *103*, 310−317.
(38) Prochazkova, S.; Vårum, K. M.; Ostgaard, K. Quantitative Determination of Chitosans by Ninhydrin. *Carbohydr. Polym.* **1999**, *38*, 115−122.
(39) Shi, L.; Caldwell, K. D. Mucin Adsorption to Hydrophobic Surfaces. *J. Colloid Interface Sci.* **2000**, *224*, 372−381.
(40) Kesimer, M.; Sheehan, J. K. Analyzing the Functions of Large Glycoconjugates through the Dissipative Properties of Their Absorbed Layers Using the Gel-Forming Mucin MUC5B as an Example. *Glycobiology* **2008**, *18*, 463−472.
(41) Deacon, M. P.; McGurk, S.; Roberts, C. J.; Williams, P. M.; Tendler, S. J.; Davies, M. C.; Davis, S. S.; Harding, S. E. Atomic Force Microscopy of Gastric Mucin and Chitosan Mucoadhesive Systems. *Biochem. J.* **2000**, *348*, 557−563.
(42) Cleary, J.; Bromberg, L.; Magner, E. Adhesion of Polyether-Modified Poly(acrylic acid) to Mucin. *Langmuir* **2004**, *20*, 9755−9762.
(43) Hagerstrom, H.; Edsman, K. Limitations of the Rheological Mucoadhesion Method: the Effect of the Choice of Conditions and the Rheological Synergism Parameter. *Eur. J. Pharm. Sci.* **2003**, *18*, 349−357.
(44) Chickering, D. E.; Mathiowitz, E. Bioadhesive microspheres: I. A Novel Electrobalance-Based Method to Study Adhesive Interactions between Individual Microspheres and Intestinal Mucosa. *J. Controlled Release* **1995**, *34*, 251−262.
(45) Takeuchi, H.; Thongborisute, J.; Matsui, Y.; Sugihara, H.; Yamamoto, H.; Kawashima, Y. Novel Mucoadhesion Tests for Polymers and Polymer-Coated Particles to Design Optimal Mucoadhesive Drug Delivery Systems. *Adv. Drug Delivery Rev.* **2005**, *57*, 1583−1594.
(46) Decuzzi, P.; Gentile, F.; Granaldi, A.; Curcio, A.; Causa, F.; Indolfi, C.; Netti, P.; Ferrari, M. Flow Chamber Analysis of Size Effects in the Adhesion of Spherical Particles. *Int. J. Nanomed.* **2007**, *2*, 689−696.
(47) Huang, Q.; Wu, H.; Cai, P.; Fein, J. B.; Chen, W. Atomic Force Microscopy Measurements of Bacterial Adhesion and Biofilm Formation onto Clay-sized Particles. *Sci. Rep.* **2015**, *5*, 16857.
(48) Iijima, M.; Yoshimura, M.; Tsuchiya, T.; Tsukada, M.; Ichikawa, H.; Fukumori, Y.; Kamiya, H. Direct Measurement of Interactions between Stimulation-Responsive Drug Delivery Vehicles and Artificial Mucin layers by Colloid Probe Atomic Force Microscopy. *Langmuir* **2008**, *24*, 3987−3992.
(49) Fischer, K. E.; Aleman, B. J.; Tao, S. L.; Hugh Daniels, R.; Li, E. M.; Bunger, M. D.; Nagaraj, G.; Singh, P.; Zettl, A.; Desai, T. A. Biomimetic Nanowire Coatings for Next Generation Adhesive Drug Delivery Systems. *Nano Lett.* **2009**, *9*, 716−720.
(50) Li, D.; Yamamoto, H.; Takeuchi, H.; Kawashima, Y. A Novel Method for Modifying AFM Probe to Investigate the Interaction between Biomaterial Polymers (Chitosan-Coated PLGA) and Mucin film. *Eur. J. Pharm. Biopharm.* **2010**, *75*, 277−283.
(51) Lehr, C.-M.; Bouwstra, J. A.; Schacht, E. H.; Junginger, H. E. In vitro Evaluation of Mucoadhesive Properties of Chitosan and Some Other Natural Polymers. *Int. J. Pharm.* **1992**, *78*, 43−48.
(52) Schaefer, D. M.; Carpenter, M.; Gady, B.; Reifenberger, R.; Demejo, L. P.; Rimai, D. S. Surface Roughness and Its Influence on Particle Adhesion Using Atomic Force Techniques. *J. Adhes. Sci. Technol.* **1995**, *9*, 1049−1062.
(53) Pettersson, T.; Dėdinaitė, A. Normal and Friction Forces between Mucin and Mucin−Chitosan Layers in Absence and Presence of SDS. *J. Colloid Interface Sci.* **2008**, *324*, 246−256.
(54) Touhami, A.; Dutcher, J. R. pH-Induced Changes in Adsorbed *β*-Lactoglobulin Molecules Measured Using Atomic Force Microscopy. *Soft Matter* **2009**, *5*, 220−227.
(55) Rief, M.; Gautel, M.; Oesterhelt, F.; Fernandez, J. M.; Gaub, H. E. Reversible Unfolding of Individual Titin Immunoglobulin Domains by AFM. *Science* **1997**, *276*, 1109−1112.
(56) Derksen, J. J.; Larsen, R. A. Drag and Lift Forces on Random Assemblies of Wall-Attached Spheres in Low-Reynolds-Number Shear Flow. *J. Fluid Mech.* **2011**, *673*, 548−573.
(57) Zeng, L.; Najjar, F.; Balachandar, S.; Fischer, P. Forces on a Finite-Sized Particle Located Close to a Wall in a Linear Shear Flow. *Phys. Fluids* **2009**, *21*, 033302.
(58) Schoenwald, R. D.; Stewart, P. Effect of Particle Size on Ophthalmic Bioavailability of Dexamethasone Suspensions in Rabbits. *J. Pharm. Sci.* **1980**, *69*, 391−394.
(59) Sieg, J. W.; Robinson, J. R. Vehicle Effects on Ocular Drug Bioavailability I: Evaluation of Fluorometholone. *J. Pharm. Sci.* **1975**, *64*, 931−936.
(60) Martín, M. J.; Calpena, A. C.; Fernández, F.; Mallandrich, M.; Gálvez, P.; Clares, B. Development of Alginate Microspheres as Nystatin Carriers for Oral Mucosa Drug Delivery. *Carbohydr. Polym.* **2015**, *117*, 140−149.
(61) Chaiyasan, W.; Srinivas, S. P.; Tiyaboonchai, W. Mucoadhesive Chitosan-Dextran Sulfate Nanoparticles for Sustained Drug Delivery to the Ocular Surface. *J. Ocul. Pharmacol. Ther.* **2013**, *29*, 200−207.


DOI: 10.1021/acsabm.8b00041
*ACS Appl. Bio Mater.* 2018, 1, 561−571

(62) Takeuchi, H.; Matsui, Y.; Yamamoto, H.; Kawashima, Y. Mucoadhesive Properties of Carbopol or Chitosan-Coated Liposomes and Their Effectiveness in the Oral Administration of Calcitonin to Rats. *J. Controlled Release* **2003**, *86*, 235−242.



DOI: 10.1021/acsabm.8b00041
*ACS Appl. Bio Mater.* 2018, 1, 561−571